

# Kenaf-Bast-Fiber-Filled Biodegradable Poly(butylene succinate) Composites: Effects of Fiber Loading, Fiber Length, and Maleated Poly(butylene succinate) on the Flexural and Impact Properties

M. Z. Ahmad Thirmizir,<sup>1</sup> Z. A. Mohd Ishak,<sup>2</sup> R. M. Taib,<sup>2</sup> S. Rahim,<sup>1</sup> S. Mohamad Jani<sup>1</sup>

<sup>1</sup>*Biocomposites and Protection Programme, Forest Research Institute Malaysia, 52109 Kepong, Selangor, Malaysia*

<sup>2</sup>*School of Materials and Mineral Resources Engineering, Seri Ampangan Engineering Campus, Universiti Sains Malaysia, 14300 Nibong Tebal, Pulau Pinang, Malaysia*

Received 10 February 2010; accepted 4 January 2011

DOI 10.1002/app.34046

Published online 7 July 2011 in Wiley Online Library (wileyonlinelibrary.com).

**ABSTRACT:** Poly(butylene succinate) (PBS) filled kenaf bast fiber (KBF) composites were fabricated via compression molding. The effects of KBF loading on the flexural and impact properties of the composites were investigated for fiber loadings of 10–40 wt %. The optimum flexural strength of the composites was achieved at 30 wt % fiber loading. However, the flexural modulus of the composites kept increasing with increasing fiber loading. Increasing the fiber loading led to a drop in the impact strength of about 57.5–73.6%; this was due to the stiff nature of the KBF. The effect of the fiber length (5, 10, 15, and 20 mm) on the flexural and impact properties was investigated for the 30 wt % KBF loaded composites. The composites with 10-mm KBF showed the highest flexural and impact properties in comparison to the others. The inferior flexural and impact strength of the composites with 15- and 20-mm KBF could be attributed to the rela-

tively longer fibers that underwent fiber attrition during compounding, which consequently led to the deterioration of the fiber. This was proven by analyses of the fiber length, diameter, and aspect ratio. The addition of maleated PBS as a compatibilizer resulted in the enhancement of the composite's flexural and impact properties due to the formation of better fiber–matrix interfacial adhesion. This was proven by scanning electron microscopy observations of the composites' fracture surfaces. The removal of unreacted maleic anhydride and dicumyl peroxide residuals from the compatibilizers led to better fiber–matrix interfacial adhesion and a slightly enhanced composite strength. © 2011 Wiley Periodicals, Inc. *J Appl Polym Sci* 122: 3055–3063, 2011

**Key words:** biodegradable; compatibilization; composites; fibers; mechanical properties

## INTRODUCTION

Currently, the development of biocomposites that are based on a combination of biodegradable polymers and lignocellulosic fibers is being widely explored. Efforts to produce biodegradable polymers are being intensively undertaken, and some specific grades of biodegradable plastics are being commercialized to promote and expand the utilization of biodegradable polymers. Poly(butylene succinate) (PBS) is a biodegradable, aliphatic, thermoplastic polyester.<sup>1</sup> The polymer is semicrystalline and is designed to have processability and physical properties that are similar to those of polyethylene.<sup>2</sup> PBS was claimed to undergo biodegradation during disposal in compost, moist soil, fresh water (by activated sludge), and sea-

water.<sup>1</sup> Normally, in the natural environment, a biodegradable polymer will be degraded by microorganisms to CO<sub>2</sub>, H<sub>2</sub>O, and inorganic products under aerobic conditions or to CH<sub>4</sub>, CO<sub>2</sub>, and inorganic products under anaerobic conditions.<sup>3</sup>

Lignocellulosic fibers have been chosen to replace traditional synthetic fibers such as E-glass fiber as reinforcements for thermoplastic composites because of their relatively low cost, natural biodegradability in different environments, and high specific mechanical strength and modulus.<sup>4</sup> Short-fiber-filled polymer composites were claimed to be suitable structural materials because of their high stiffness and strength-to-weight ratio, low material cost, and ability to be processed through various techniques, such as injection, compression, and transfer molding.<sup>5</sup> The molded part of the short-fiber-filled composite is highly anisotropic and has a promising homogeneous distribution of mechanical strength in all of the molding directions. To attain the maximum strength of the composite, the fiber length must be greater than a minimum value, which is called the *critical fiber length*.<sup>6</sup>

Correspondence to: Z. A. M. Ishak (zarifin.ishak@googlemail.com).

However, if the fibers are too long, they are difficult to mix well with the polymer because the fibers themselves tend to get entangled and thus restrict the flow of the molten polymer during molding.<sup>7</sup>

In natural-fiber-filled polymer composites, the poor interfacial adhesion between the fiber and the matrix is a major problem that must be overcome. This is due to the difference in polarity between the hydrophobic polymer and the hydrophilic natural fibers.<sup>8</sup> As stated by Friedrich et al.,<sup>9</sup> a strong adhesion at the fiber–matrix interface is needed to effectively transfer the load throughout the interface to the dispersed fibers. The most established method for improving the fiber–matrix interfacial adhesion is the introduction of a compatibilizer that contains bifunctional groups, which are capable of attaching to the fiber's surface and the polymer phase. Maleated polyolefins, such as maleated polypropylene and maleated polyethylene, are commercially used in the composite industry.<sup>10</sup>

However, few studies have been reported on the grafting process for the maleated polyester compatibilizer. An attempt to graft maleic anhydride (MA) onto PBS was reported by Mani et al.<sup>11</sup> through a study on the functionalization of a biodegradable polyester with MA by reactive extrusion. There are several other techniques that can be applied to produce a maleated compatibilizer; these are known as the solvo-grafting and the solid phase-grafting techniques.<sup>12</sup> Normally, the grafting of MA onto polymer chains is conducted through a reactive melt-mixing technique in the presence of a peroxide initiator [e.g., benzoyl peroxide, dicumyl peroxide (DCP), azobis(isobutyronitrile), and di-*tert*-butyl peroxide].<sup>13,14</sup> The purposes of this study were (1) to investigate the effect of the fiber length, diameter, and aspect ratio distribution on the properties of PBS/kenaf bast fiber (KBF) composites; (2) to produce and characterize maleated poly(butylene succinate) (PBSgMA) compatibilizers; and (3) to determine the effect of purified and unpurified compatibilizer addition on the mechanical properties of PBS/KBF composites.

## EXPERIMENTAL

### Materials

KBF in predetermined lengths of 5, 10, 15, and 20 mm was supplied by Kenaf Fibre Industries (Malaysia). PBS, which is also known as Bionolle, has a melt flow index of 26 g/10 min (at 130°C and 2.16 kg load) and a density of 1.26 g/cm<sup>3</sup>; it was supplied by Showa Highpolymer (Japan).

### Preparation of the PBSgMA compatibilizer

Reactive mixing of the PBSgMA compatibilizer was carried out with an internal mixer with corotating

**TABLE I**  
Formulation of the PBSgMA Compatibilizer

PBSgMA	Part per hundred (phr)		
	PBS	MA	DCP
3PBSgMA	100	3	1
5PBSgMA	100	5	1
7PBSgMA	100	7	1
10PBSgMA	100	10	1

double-winged rotors (model Brabender internal mixer) at 140°C with a 50-rpm rotor speed for a total mixing time of 5 min. Before they were fed into the compounding chamber, PBS, DCP, and MA were thoroughly premixed in a plastic container. Four formulations of compatibilizer were introduced, as shown in Table I.

### Purification

In this study, two different series of compatibilizers were introduced; unpurified PBSgMA and purified maleated poly(butylene succinate) (pPBSgMA) compatibilizers. For pPBSgMA, the grafted polymer was refluxed in chloroform for 1 h; then, the hot solution was poured into cool methanol and filtered. The precipitated polymer was then further washed with fresh methanol to remove the unreacted MA and the DCP residues. Finally, the polymer was dried in a circulating air oven at 80°C for 24 h. The compatibilizer was kept in a sealed plastic bag before use.

### Determination of the MA content

The anhydride content of the grafted polymer was determined by titration of the acid groups derived from the anhydride's functional groups; the method was suggested by Zhu et al.<sup>15</sup> In this method, 1 g of pPBSgMA compatibilizer was dissolved in 100 mL of refluxing chloroform for 30 min. Then, 5 mL of distilled water was added to the hot solution to hydrolyze the anhydride groups. Immediately, the hot solution was titrated against 0.025N ethanolic KOH in the presence of four drops of 1% phenolphthalein in ethanol, which was used as the indicator. The titration was stopped once the purple end point was reached. A blank titration was also carried out by the same method as the compatibilizers. The grafting degree of MA to PBS was calculated with eq. (1):

$$\text{Grafting degree of MA} = \frac{98.06c(V - V_0)}{2 \times 1000m} \times 100\% \quad (1)$$

where  $V$  and  $V_0$  (mL) represent the volumes of the KOH/C<sub>2</sub>H<sub>5</sub>OH solution that were used for titration of the grafted and blank samples, respectively;  $c$  is

TABLE II  
Effect of the KBF Loading on the Flexural and Impact Properties of the PBS/KBF Composites

Fiber loading (wt %)	Flexural properties		Impact strength (J/m <sup>2</sup> )
	Flexural strength (MPa)	Flexural modulus (GPa)	
0	36.54 ± 0.63	0.62 ± 0.01	39.52 ± 3.24
10	36.83 ± 1.92	1.16 ± 0.13	16.80 ± 0.92
20	37.33 ± 0.80	2.58 ± 0.08	13.08 ± 0.46
30	40.21 ± 0.68	3.04 ± 0.18	10.68 ± 0.67
40	38.04 ± 0.78	3.25 ± 0.12	10.44 ± 0.31

the molar concentration of the KOH/C<sub>2</sub>H<sub>5</sub>OH solutions (mol/L); 98.06 (g/mol) is the molecular weight of MA; *m* (g) is the weight of the compatibilizer; and the number 2 indicates that one anhydride group could change into two carboxylic groups after the rings of the MA were opened.

### Preparation of the composites

KBF and PBS were dried in a circulating air oven at 80°C for 16 h and were kept in desiccators before processing. The composites were prepared with an internal mixer with corotating double-winged rotors. The temperature of the compounding chamber was set at 130°C. Generally, the temperature of the chamber was allowed to stabilize for approximately 3 min before it was loaded with PBS pellets. For the compounding of the compatibilized composite, the PBS and PBSgMA were physically premixed before they were fed into the chamber. Then, the fiber was gradually added to the chamber under a low rotor speed (10 rpm). Once all of the fiber was fed, the compounding process was continued at a rotor speed of 50 rpm for 5 min before it was discharged. The composite compounds were compression-molded at 130°C into specimens with dimensions of 120 × 12 × 3 mm<sup>3</sup> and 64 × 12 × 4 mm<sup>3</sup> for flexural and impact tests, respectively, with a compression-molding machine Kao Teih Gotech (Guangdong, China). The molding cycle involved 5 min of preheating without pressure, 3 min of compression under 150 kg/cm<sup>3</sup> of pressure, and 5 min of cooling under the same pressure. Before testing, the molded specimens were kept in desiccators and conditioned at room temperature for at least 24 h.

### Determination of the fiber length and diameter distribution

Measurement of the KBF length and diameter before and after compounding was done with a stereozoom microscope SXGA, VWR international (Radnor, PA) that was equipped with image analysis software (VIS Plus version 2.90). The precut KBF's (5, 10, 15, and 20 mm) length and diameter were measured directly with a stereozoom microscope. Fibers from the com-

pounded composites were isolated by dissolution of the composites in chloroform. The fibers were then rinsed thoroughly and dried for 24 h at 70°C. Before measurement, the fibers were spread out and placed between the microscope's glass slides before they were viewed under the microscope. The fibers were viewed at a resolution of 4800 dpi; the fiber lengths and diameters were measured with the VIS Plus software with a precalibrated measuring scale. At least 200 fibers were measured for each targeted KBF length; their lengths and diameters were statistically analyzed and presented in distribution curves.

### Flexural and impact tests

Flexural testing was carried out in accordance with ASTM D 790-98 with a universal testing machine that was equipped with a control system series IX model Instron 3366 (Norwood, MA) and a 10-kN load cell. The crosshead speed was set at 5 mm/min. Five specimens were tested for each series. The Izod impact strength for the unnotched specimens was determined in accordance with ASTM D 256-97. The impact test was carried out with a digital pendulum impact tester (model Gotech) and a 7.5-J pendulum. Ten specimens were tested for each formulation. All of the tests were done at room temperature.

### Morphological observation

We conducted a morphological study of the flexural fracture surface by taking scanning electron micrographs at an acceleration voltage of 25 kV at predetermined magnifications in a low-vacuum-mode scanning electron microscope FEI Quanta 200 (Hillsboro, OR). The specimens were observed as prepared. The morphological study of the fracture surfaces was conducted to study the failure mechanism and to observe both the PBS resin and the KBF interfacial adhesion.

## RESULTS AND DISCUSSION

### Effect of fiber loading

Flexural and impact properties

Table II shows the effect of KBF loading on the flexural properties of the PBS and PBS/KBF composites.

**TABLE III**  
Average Fiber Length ( $L$ ), Average Fiber Diameter ( $D$ ), and Aspect Ratio ( $L/D$ ) of the KBF Before and After Compounding

Designation	Before compounding			After compounding		
	$L$ (mm)	$D$ (mm)	$L/D$	$L$ (mm)	$D$ (mm)	$L/D$
5-mm KBF	6.90	0.10	69.00	0.77	0.07	9.63
10-mm KBF	11.77	0.09	130.78	0.82	0.08	10.25
15-mm KBF	15.74	0.10	157.4	0.74	0.09	8.22
20-mm KBF	21.68	0.09	240.89	0.86	0.09	9.56

Generally, the flexural strength of the PBS/KBF composites was higher than that of the neat PBS. An increase in the KBF loading improved the flexural strength of the composites. This indicated that incorporation of more KBF increased the composite's flexural strength. According to Shibata et al.,<sup>16</sup> KBF can be classified as a reinforcement filler because of its inherent properties, such as a high stiffness and strength. Perhaps the enhanced flexural strength was also due to the incorporated fibers, which had a sufficiently high aspect ratio, which allowed mechanical interlocks to form between the fiber and the matrix. The fiber–matrix mechanical interlocking was expected to act as a mechanism for the composites to withstand the bending force. The collapsing of the fiber–matrix interfacial gaps upon bending was expected to allow better contact between the matrix and the embedded fibers.<sup>5</sup> This physical interaction allows the applied load to be transferred to the fibers via mechanical shearing at the fiber–matrix interface. However, the physical interactions gradually decrease with the extent of matrix deformation because the stretched matrix cannot grip the fibers efficiently, which thus allows the fibers to loosen and slip until failure. The flexural strength of the composites increased up to an optimum fiber loading of 30 wt %; it then decreased with further increases in the KBF loading. Perhaps at a higher fiber loading than the optimum fiber loading, the incorporated fibers tended to agglomerate between the neighboring fibers and, thus, weakened the composites.<sup>17</sup>

The flexural modulus of the PBS/KBF composites was higher than that of the neat PBS because of the stiffening effect of the incorporated KBF. As shown in Table II, the flexural modulus of the composites increased proportionally to the KBF loading; the increases ranged from 87.1 to 429.2%. This was typical behavior for natural-fiber-filled thermoplastic composites because the stiffness of the composites increased with the fiber fraction.<sup>18</sup> Several studies also reported increases in the flexural modulus with increases in the filler loading in plastic composites.<sup>3,17,18</sup>

Table II also presents the effect of fiber loading on the impact strength of the PBS/KBF composites. Because unnotched specimens were used in this

study, the impact strength values are measurements of the energy that was used by the composites to initiate and propagate the crack until failure.<sup>17</sup> From the results, the impact strength of the PBS/KBF composites was lower than that of the neat PBS. The drop in the impact strength with increases in the fiber loading ranged from 71 to 81%. With incorporation of the KBF, an abrupt change in the impact strength was associated with a change in the composite's failure mode from ductile to brittle behavior. This is a common observation for lignocellulosic-fiber-filled polymer composites because the presence of fibers restrict the matrix phase mobility and, thus, reduce the capability of the composite to absorb energy during failure.<sup>2</sup> Once the crack was initiated, the energy continued to be absorbed by the work of crack propagation, which was due to either matrix-related or fiber-related energy absorbing mechanisms.<sup>17</sup> In addition, the incompatibility issue between the hydrophobic matrix and the hydrophilic fiber caused the impact energy absorbing capability to be poorer in the composites because of the existence of bordered pits at the fiber–matrix interface, which tended to restrict stress transfer from the matrix phase to the incorporated fibers.<sup>2</sup>

### Effect of the fiber length

Analysis of the fiber length and diameter distributions

Table III presents the average fiber length and diameter and the aspect ratio for each targeted KBF length, that is, 5, 10, 15, and 20 mm before and after compounding. It can be seen that the average fiber lengths before compounding were close to the targeted fiber length. This indicated that the fiber cutting was reliable to produce acceptable ranges of fiber lengths. However, the average length for each targeted fiber length after composite compounding converged to lower values, which ranged from 0.74 to 0.86 mm. This showed that the melt compounding process resulted in fibers breaking into smaller pieces because of the strong shear stresses of the viscous molten polymer, which developed in the compounding chamber.<sup>4,19</sup>

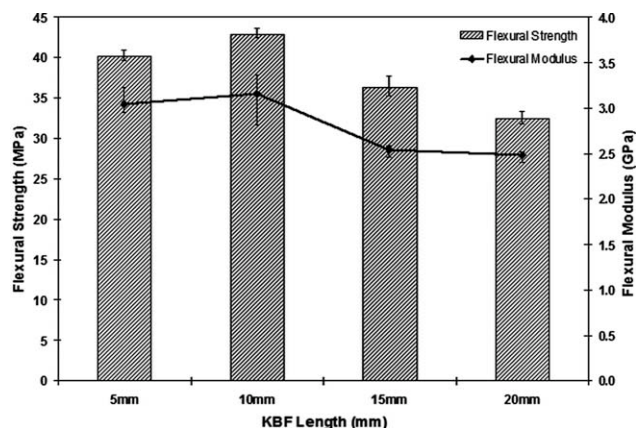


**Figure 1** Effect of the fiber length on the flexural properties of the PBS30KBF composites.

As seen in Table III, the values of the fiber diameters for each targeted fiber length seemed to shift slightly to a lower range after compounding, from 0.09–0.10 to 0.08–0.09 mm, respectively. The drop in the fiber diameters could have been due to fibrillation of the fiber bundles into elementary fibers because of the high mechanical shearing that developed in the compounding chamber.<sup>19</sup> As a result, the fiber aspect ratios for all of the targeted fiber lengths also decreased and converged to lower values, which ranged from 8.2 to 10.3, as a result of serious fiber breakage and fibrillation during the compounding process.<sup>4,19</sup> Perhaps the longer targeted fiber length was the more severe fiber damage and the higher percentage drop in the aspect ratio.

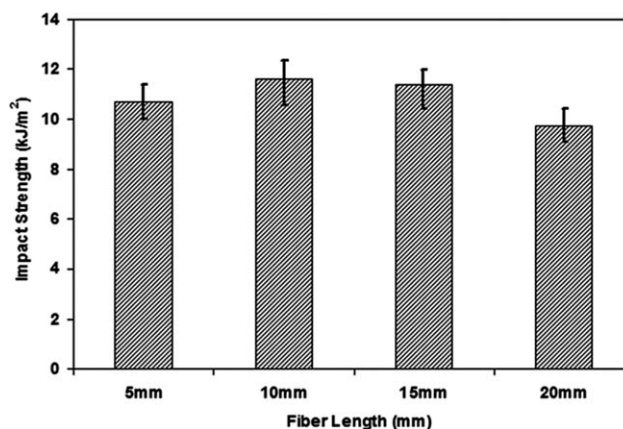
#### Effect of the KBF fiber length on the flexural and impact properties of the PBS/KBF composites

Figure 1 shows the effect of the fiber length on the flexural strength of the PBS/KBF composites at 30 wt % fiber loading (PBS30KBF). The highest increment of about 6.7% in the flexural strength was achieved in the composite with the addition of 10-mm KBF. The flexural strength of the PBS30KBF composites with the addition of 15- and 20-mm KBF decreased by 9.6 and 19.5%, respectively, in comparison to the reference composite (the PBS30KBF composite with 5-mm KBF). This result indicates that the addition of KBF with fiber lengths longer than 10 mm did not produce any promising reinforcing effects in the PBS/KBF composites. As mentioned previously, the longer KBF resulted in severe fiber breakage and fibrillation during composite compounding. As the fiber length increased, the fragmentation and damage that occurred to the fibers became more severe.<sup>4,6</sup> The severe damage of the fibers that was caused by the high mechanical shearing that developed in the compounding chamber

was expected to reduce the fiber's stiffness and strength.

Figure 1 shows the effect of the fiber length on the flexural modulus of the PBS/KBF composites. A small increment in the flexural modulus was obtained in composites with the addition of 10- and 15-mm KBF. This may have been due to the remaining of reinforcing effect of the fibers that was not deteriorated by the action of mechanical shearing. However, for composites with the addition of 10-mm KBF, the increase in the flexural modulus was accompanied by a 6.7% increase in the flexural strength of the composites. On the other hand, for composites with 15-mm KBF, the increase in the flexural modulus was accompanied by a reduction in the flexural strength of about 10%; this was due to severe fiber attrition during compounding.

As shown in Figure 1, tremendous drops in the flexural modulus of about 16.4 and 18.4% were observed for those composites incorporated with 15- and 20-mm KBF, respectively. The relatively poor stiffening effect of the KBF in those cases could have been related to severe fiber attrition, which contributed to reducing the aspect ratio.<sup>6,20</sup> In addition, the incorporation of long fibers (in this case, fibers with lengths of 15 and 20 mm) was also expected to result in poor fiber dispersion and to promote unwanted fiber entanglement and, thus, resulted in inferior properties of the composites. On the basis of these results, the PBS30KBF composite with 10-mm KBF was considered to be the best formulation for the PBS/KBF composite system. As seen in Figure 2, the composite with 10-mm KBF had an 8.5% greater impact strength. In contrast, the composite with the 20-mm fiber length had an 8.6% poorer impact strength. The decrease in the impact strength could have been due to the severe fiber damage that resulted from composite compounding.<sup>6</sup>



**Figure 2** Effect of the fiber length on the impact strength of the PBS30KBF composites.

**TABLE IV**  
Effect of the MA Content on the Percentage of MA Grafting of PBS

PBSgMA compatibilizer	Content of MA (phr)	Grafting degree (%)
3pPBSgMA	3	0.91 ± 0.03
5pPBSgMA	5	1.07 ± 0.02
7pPBSgMA	7	2.14 ± 0.04
10pPBSgMA	10	2.32 ± 0.05

### Effect of PBSgMA on the PBS/KBF composites

#### Synthesis and characterization of PBSgMA

From early observations of the purification of PBSgMA, all of the compatibilizers seemed to fully dissolve in refluxed chloroform because no crosslinking reaction took place during the grafting process.<sup>20</sup> According to Mani et al.,<sup>11</sup> the grafting process that was initiated by the peroxide possibly caused the occurrence of the unwanted crosslinking reaction between the polymer chains, especially for the grafting reaction that involved a high concentration of initiator. The graft content of the compatibilizers was controlled by many factors: the monomer and initiator concentrations, reaction temperature, rotor speed, and residence time.<sup>21</sup> However, for this study, all of the processing parameters were fixed, and only the content of MA was varied according to the predetermined formulations, as shown in Table I.

As shown in Table IV, the grafting degree of the pPBSgMA compatibilizers increased as the MA contents increased. As stated by Mani et al.,<sup>11</sup> increasing the MA content led to an increase in the percentage of grafting because of the greater chances of the MA group attaching to the radical sites during the reaction. However, there was a possibility for chain scission to occur during the reaction, which thus resulted in a reduction in the intrinsic viscosity of the compatibilizer. As suggested by Mani et al.,<sup>11</sup> the grafting degree was directly influenced by the concentration of the initiator because it controlled the amount of radical sites that were created on the PBS chains. An increase in the MA concentration increased the amount of anhydride group in the compatibilizers and, thus, enhanced the efficiency of grafting by reducing the probability of radical termination before the grafting of MA onto the PBS chains took place.<sup>11</sup> To determine the optimum MA concentration that was suitable for this compatibilizer system, the compatibilized composites were directly assessed with flexural and impact tests.

#### Effect of PBSgMA addition on the PBS/KBF composites

The effect of the addition of compatibilizer on the flexural and impact properties of the PBS/KBF composites was studied at a fiber loading of 30 wt % and a fiber length of 10 mm. The effect of the unpurified PBSgMA and pPBSgMA compatibilizers on the flexural strength of the composites is shown in Figure 3. It could be seen that the PBS/KBF composites compatibilized with pPBSgMA had a higher flexural strength than the uncompatibilized composite (control). In the case of the unpurified PBSgMA, only the composites with the addition of 3PBSgMA and 5PBSgMA (The numbers before PBSgMA refer to the concentration of maleic anhydride (MA) in the compatibilisers) showed superior flexural strength in comparison to the control composite, and the increases were about 2.7 and 7.4%, respectively. The increases in the flexural strength with the addition of the both compatibilizers could have been associated with the improvement of the fiber–matrix interfacial adhesion. According to Tserki et al.,<sup>21</sup> the improvement in the fiber–matrix interfacial adhesion was attributed to the ability of the MA to react with the hydroxyls group of the lignocelluloses and the good compatibility of the grafted copolymer chains with the main polymeric phase. On the contrary, the inferior flexural strength of the composites with the addition of 7PBSgMA and 10PBSgMA was probably due to the presence of high contents of ungrafted MA residue and the severe chain scissions of the PBS during the grafting process.<sup>11</sup>

It was interesting to note that the composites with added unpurified and purified compatibilizers achieved optimum flexural strength with increases of about 7.4 and 12.7% when the compatibilizers had a 5-phr concentration of MA. On the basis of the optimum increment in the flexural strength, the 5pPBSgMA compatibilizer could be considered to be the ideal compatibilizer for the PBS/KBF composites. Mani et al.<sup>11</sup> suggested that the ideal compatibilizer must achieve an optimum degree of grafting with minimal polymer chain degradation and contribute to significant enhancements in the fiber–matrix

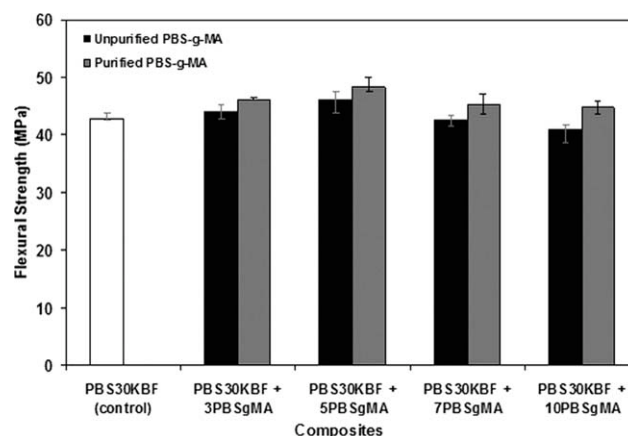


**Figure 3** Effect of pPBSgMA and unpurified PBSgMA on the flexural strength of the PBS30KBF composites.

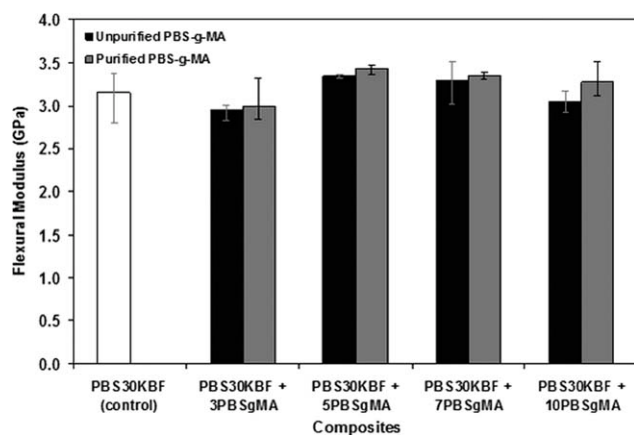


**Figure 4** Effect of pPBSgMA and unpurified PBSgMA compatibilizer on the flexural modulus of the PBS30KBF composites.

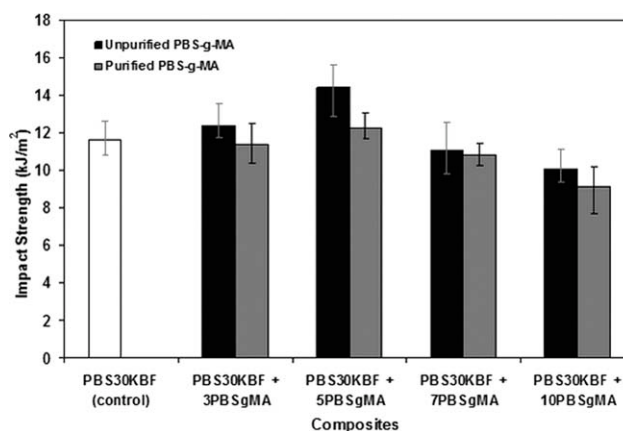
interfacial adhesion. As shown in Figure 3, the flexural strength of the composites that were compatibilized with unpurified compatibilizers were relatively lower than that of the composites compatibilized with purified compatibilizers. Perhaps the residuals of the ungrafted MA and the unreacted DCP initiator that were present in the compatibilizers might have acted as stress concentrators because of its poor interaction with the constituent materials.<sup>13</sup> This showed that the purification process was essential in producing good quality compatibilizers without the presence of any unreacted residues. Bettini and Agnelli<sup>13</sup> also stated that the residual of the MA could not be removed by self-evaporation during melt grafting if the reaction was conducted at lower temperatures than the boiling point of the MA (202°C). In this study, the grafting reaction was carried out at about 140°C, which was far lower than the boiling point of MA; thus, the residual of the MA still remained in the compatibilizer mixture.

As seen in Figure 4, both of the composites that incorporated the 3PB SgMA and 3pPBSgMA compatibilizers had a slightly lower flexural modulus than the control composite. However, further increases in the MA concentration in the compatibilizers resulted in moderate increments in the flexural modulus of the composites. The maximum increase in the composite's flexural modulus for each series of the compatibilizer was at a MA concentration of 5 phr. The increases were 6.0 and 8.9% for composites with unpurified and purified compatibilizers, respectively. Further increases in the MA concentration, that is, 7 and 10 phr in the compatibilizers, revealed a slight decrease in the flexural modulus. However, the flexural modulus of the composites with purified compatibilizers were higher than that of the control composite. The reduction is believed to be due to a decrease of the compatibilizer intrinsic strength resulting from severe chain scission during the grafting process with the presence of a high concentration of MA,<sup>11</sup>

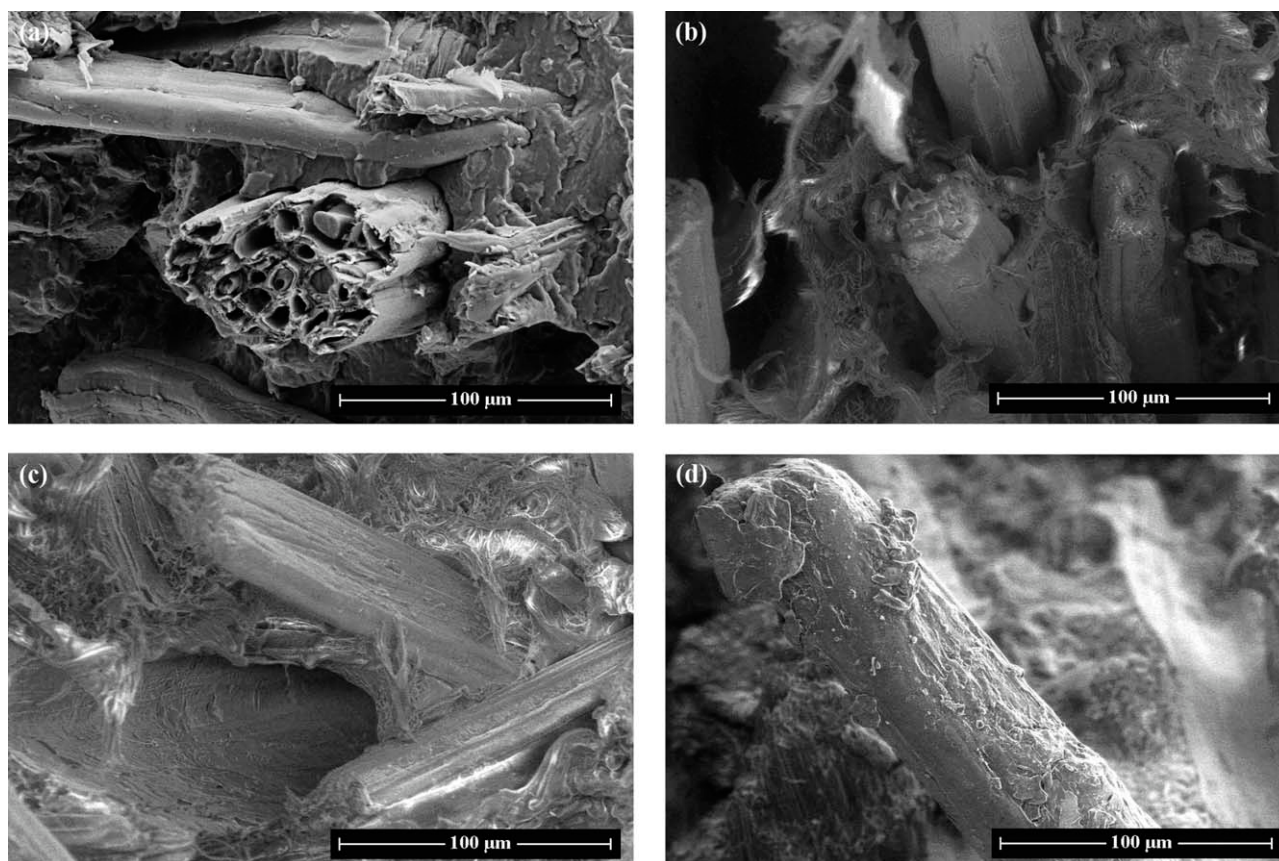
although the decrease in the flexural modulus at a 10-phr MA concentration of compatibilizer observed in composites compatibilized with unpurified compatibilizer was due to the relatively poor fiber–matrix interfacial adhesion, which resulted from severe chain scission of the grafted polymer and the presence of a high content of ungrafted MA residue in the compatibilizers.<sup>11</sup> On the contrary, all of the composites with the addition of purified compatibilizers had a superior flexural modulus in comparison to those composites with the addition of unpurified compatibilizers because of the elimination of MA residue from the compatibilizer mixture by the purification process. The observed trend confirmed that the elimination of ungrafted MA led to better fiber–matrix interfacial adhesion.<sup>11</sup>

Figure 5 shows the effect of the pPBSgMA and unpurified PBSgMA on the Izod impact strength of the PBS30KBF composites. For the composites with unpurified compatibilizers, increments in the impact strength of about 6.6 and 24.2% were observed for the composites with the 3PB SgMA and 5PB SgMA compatibilizers, respectively. The addition of unpurified compatibilizer with a MA concentration that was higher than 5 phr resulted in a lower impact strength. A similar trend was also observed for the composites that were compatibilized with pPBSgMA, where the optimum impact strength was achieved with the 5-phr MA concentration. However, the values were slightly lower in comparison to those composites with unpurified compatibilizers. The low impact strength of the composites with the purified compatibilizers could have been related to the elimination of the unreacted residues (MA and DCP) during purification process. The elimination of the residues led to a cohesive fiber–matrix interaction and an enhanced composite strength, as indicated by the superior flexural strength of the composites.

In addition, the presence of MA side grafting on the PBS backbone tended to reduce the mobility of



**Figure 5** Effect of pPBSgMA and unpurified PBSgMA compatibilizer on the impact strength of the PBS30KBF composites.



**Figure 6** SEM micrographs of the PBS30KBF composite's fracture surfaces: (a) control, (b) with unpurified compatibilizer (5PBsgMA), (c) with pPBsgMA compatibilizer (5pPBsgMA), and (d) fiber pullout that appeared on the fracture surface of PBS30KBF with the 5pPBsgMA compatibilizer.

the PBS chain.<sup>10</sup> The addition of the maleated compatibilizer to the composites also possibly caused mechanical interlocking between the fibers and the compatibilizer or/and between the polymer chains and the compatibilizer. The interlocking interaction may have concurrently existed across the interface at various degrees.<sup>10</sup> The effect of the interlocking interaction was more pronounced for the composites with purified compatibilizer because the removal of the MA residue from the compatibilizer led to closer packing of the MA-grafted PBS chains; in addition, the presence of grafted MA groups in the compatibilizer tended to restrict the segmental motion of the PBS matrix.<sup>10</sup> In the case of unpurified PBsgMA, the presence residual of MA could have served as spacers between the PBS chains and, thus, facilitated the chains sliding upon subjection to impact force. This allowed higher impact energy was absorbed during the failure process.

#### Scanning electron microscopy (SEM) micrograph

As can be seen in Figure 6(a), the fiber bundle clearly appeared on the composite's fracture surface. This result was in agreement with the recent work

by Ochi,<sup>22</sup> where the kenaf fiber bundle appeared as a group of elementary fibers that were bonded together. The presence of the fiber bundles in the composites was expected to promote interfibrillar voids between the elementary fibers and, thus, contribute toward premature failure of the composites.<sup>23</sup> It is known that KBF usually results in irregular surface roughness and dimensions. Besides, the fibers also tend to coil and kink during the compounding process, and due to the strong shear stresses that develop in the viscous molten polymer, the fibers also break and fibrillate into smaller pieces.<sup>4</sup>

The difference in the polarity between the hydrophilic lignocellulosic fiber and the hydrophobic polymer matrix resulted in a lack of interfacial adhesion between the composite's constituents.<sup>2</sup> The formation of gaps that surround the fibers, as shown by the SEM micrographs in Figure 6(a), provided evidence of poor fiber–matrix interfacial adhesion between the KBF and the PBS. The poor fiber–matrix adhesion reduced the strength of the composite because the applied stresses would have not been successfully transferred to the dispersed fibers.<sup>4</sup> It also can be seen that the interfacial gaps between the fiber and matrix shown in Figure 6(a) were



larger than those shown in Figure 6(b) and 6(c). This clearly indicates the lack of fiber–matrix interfacial adhesion in the control composite. An improvement in the interfacial adhesion was observed for the PBS30KBF composite with both the 5PBSgMA and 5pPBSgMA compatibilizers [refer to Fig. 6(b,c)]. A well-defined fiber–matrix adhesion without the gap formation was observed at the composite fiber–matrix interface. As shown by Figure 6(d), the fiber pullout that was observed on the composite fracture surface was coated by the PBS matrix. This indicated that the addition of PBSgMA was effective in improving the interfacial adhesion between the PBS and KBF. On the contrary, as shown by Figure 6(a), the smooth fiber surface without traces of matrix adhesion was observed on the fracture surface of the PBS30KBF composite. This confirmed the poor adhesion between the hydrophobic PBS matrix and the hydrophilic KBF due to differences in polarity between these two components.

### CONCLUSIONS

The optimum fiber loading for the PBS/KBF composite was 30 wt %, as reflected by the highest flexural strength of the composites, that is, about 40 MPa. Further study on the effect of fiber length showed the optimum flexural and impact properties were achieved with the addition of 10-mm KBF. Both the pPBSgMA and unpurified PBSgMA compatibilizers with a concentration MA of 5 phr were found to be effective in improving the fiber matrix interfacial adhesion and, thus, improved the mechanical properties of the PBS/KBF composites. Purified compatibilizer with a 5-phr concentration of MA (5pPBSgMA) was considered to be the best compatibilizer suited to this PBS/KBF composites with promising significant enhancement in the composite flexural strength and modulus of 13 and 9%, respectively. The removal of the unreacted MA and

DCP residues by the purification process was also essential to improve fiber–matrix interfacial adhesion and, thus, enhance the composite's properties.

### References

1. Fujimaki, T. *Polym Degrad Stab* 1998, 59, 209.
2. Kim, H. S.; Yang, H. S.; Kim, H. J. *J Appl Polym Sci* 2005, 97, 1513.
3. Arvanitoyannis, I.; Biliaderis, C. G.; Ogawa, H.; Kawasaki, N. *Carbohydr Polym* 1998, 36, 89.
4. Baiardo, M.; Zini, E.; Scandola, M. *Compos Appl Sci Manuf* 2004, 35, 703.
5. Chen, C. Y.; Tucker, C. L. *Reinforced Plast Compos* 1984, 3, 120.
6. Facca, A. G.; Kortschot, M. T.; Yan, N. *Compos Appl Sci Manuf* 2006, 37, 1660.
7. Nystrom, B.; Joffe, R.; Langstrom, R. *Reinforced Plast Compos* 2007, 26, 579.
8. Khan, M. A.; Bhattacharia, S. K. *Reinforced Plast Compos* 2007, 26, 617.
9. Friedrich, M.; Christian, F.; Heinz, H. *Processing of Bast Fibre Plants for Industrial Application. Natural Fibre, Biopolymers and Biocomposites*; Taylor & Francis: New York, 2005.
10. Keener, T. J.; Stuart, R. K.; Brown, T. K. *Compos Appl Sci Manuf* 2004, 35, 357.
11. Mani, R.; Bhattacharya, M.; Tang, J. *Polym Sci Part A: Polym Chem* 1999, 37, 1693.
12. Qiu, W.; Endo, T.; Hirotsu, T. *Eur Polym* 2005, 41, 1979.
13. Bettini, S. H. P.; Agnelli, J. A. M. *Polym Test* 2000, 19, 3.
14. Kalambur, S.; Rizvi, S. S. *J Plast Film Sheeting* 2006, 22, 39.
15. Zhu, L.; Tang, G.; Shi, Q.; Cai, C.; Yin, J. *React Funct Polym* 2006, 66, 984.
16. Shibata, S.; Cao, Y.; Fukumoto, I. *Compos Appl Sci Manuf* 2008, 39, 640.
17. Mohd Ishak, Z. A.; Yow, B. N.; Ng, B. L.; Khalil, H. P. S. A.; Rozman, H. D. *Appl Polym Sci* 2001, 81, 742.
18. Shibata, S.; Cao, Y.; Fukumoto, I. *Polym Test* 2005, 24, 1005.
19. Bos, H. L.; Mussig, J.; Van Den Oever, M. J. A. *Compos Appl Sci Manuf* 2006, 37, 1591.
20. Liu, W.; Drzal, L. T.; Mohanty, A. K.; Misra, M. *Compos Eng* 2007, 38, 352.
21. Tserki, V.; Matzinos, P.; Panayiotou, C. *Compos Compos Appl Sci Manuf* 2006, 37, 1231.
22. Ochi, S. *Mech Mater* 2008, 40, 446.
23. Nishino, T.; Hirao, K.; Kotera, M.; Nakamae, K.; Inagaki, H. *Compos Sci Tech* 2003, 63, 1281.